Letter

Contrarian role of phase and phase velocity coupling in synchrony of second-order phase oscillators

Arindam Mishra,[1] Suman Saha,[2,*] Subrata Ghosh,[3,*] Syamal Kumar Dana,[4,5] and Chittaranjan Hens[3]

[1]*Department of Physics, National University of Singapore, Singapore 117551, Singapore*
[2]*National Brain Research Centre, Manesar, Gurugram 122051, India*
[3]*Center for Computational Natural Sciences and Bioinformatics, International Institute of Information Technology, Gachibowli, Hyderabad 500 032, India*
[4]*Department of Mathematics, Jadavpur University, Kolkata 700032, India*
[5]*Division of Dynamics, Lodz University of Technology, 90-924 Lodz, Poland*

(Received 8 March 2023; accepted 2 October 2023; published 26 October 2023)

Positive phase coupling plays an attractive role in inducing in-phase synchrony in an ensemble of phase oscillators. Positive coupling involving both amplitude and phase continues to be attractive, leading to complete synchrony in identical oscillators (limit cycle or chaotic) or phase coherence in oscillators with heterogeneity of parameters. In contrast, purely positive phase velocity coupling may originate a repulsive effect on pendulumlike oscillators (with rotational motion) to bring them into a state of diametrically opposite phases or a splay state. Negative phase velocity coupling is necessary to induce synchrony or coherence in the general sense. The contrarian roles of phase coupling and phase velocity coupling on the synchrony of networks of second-order phase oscillators have been explored here. We explain our proposition using networks of two model systems, a second-order phase oscillator representing the pendulum or the superconducting Josephson junction dynamics, and a voltage-controlled oscillations in neurons model. Numerical as well as semianalytical approaches are used to confirm our results.

DOI: 10.1103/PhysRevE.108.L042201

Depending on the length of the bob, a forced pendulum may reveal qualitatively distinct periodic orbits. For instance, investigations suggest [1,2] that shortening the length of a pendulum leads to *rotational* motion, in which the external torque rotates the pendulum in full swing, i.e., 360°. On the other hand, motion is confined to nonoverturning motion if the length of the pendulum is increased beyond a critical value. This is called *librational* motion. The motion of such an isolated pendulum is captured by two variables: ϕ describes the phase angle, and $\dot{\phi}$ reflects the phase velocity (or frequency). This description is equivalently mapped in the superconducting Josephson junction [3–12] and the sine-Gordon equation [13]. In particular, in a Josephson junction, the phase velocity variable evolves as the voltage across the junction that is proportional to the frequency variable. In this setup, several investigations suggest that a chain of such pendula may reveal spatiotemporal chaos if there is specific heterogeneity in the model, and may emerge at a high degree of complete synchronization if there is strong positive coupling through the phase variable [1,2,14,15]. A key observation of the emergence of complete synchronization (CS) in such systems relies on the fact that the system is in rotational motion and attractive positive coupling is always applied involving the phase variables. By contrast, in an array of classical Josephson junctions (see the model $\mathcal{M}_1$, Fig. 1), in which the system exhibits rotational motion, negative coupling is essential for the realization of CS if the coupling is applied using a voltage (phase velocity) variable [16]. In earlier investigations, it was observed that the oscillators may also arrive at a state of out-of-phase synchrony or a splay state [17,18] for positive voltage coupling. Negative voltage coupling is a necessity for the realization of in-phase coherence in nonidentical junctions (CS in the identical case) if the system reveals rotational motion (see the model $\mathcal{M}_1$, Fig. 1). Such negative voltage coupling was used in earlier studies [17,19] for the realization of stable coherent dynamics, but never categorically discussed regarding the repulsive effect of voltage coupling. The information was hidden within the mathematical formulation and missed the attention of researchers until recently [5,16,20,21].

Thus, the conventional paradigm [22–32] of synchrony, in which a usual second-order (continuous) synchronization transition occurs under positive phase/amplitude coupling, drastically fails in arrays of oscillators with a second-order pendulumlike dynamics if it is connected with phase velocity or voltage coupling.

Motivated by these observations, we study the impact of phase and phase velocity (or voltage) coupling in a class of pendulumlike models (see the models in Fig. 1) that show either librational or rotational motion. The phase velocity (or voltage) and phase variables appear disparately in the model description. To decipher our observation [16,20], we explore the impact of phase and phase velocity coupling separately, using a semianalytical approach and more rigorous numerical studies, on an array of the second-order phase model that represents the Josephson junction dynamics. Furthermore, we explore a network of a voltage-controlled oscillations in neurons (VCON) model [33,34] that is also described by another second-order phase model and shows either *rotation* or

*Corresponding authors: ecesuman06@gmail.com; jaba.subrata94@gmail.com

Model	**Coupled Model Equations**	**Range of Parameters ($\epsilon_1 = 0$, $\epsilon_2 = 0$)**		**Libration ($\epsilon_1 = 0$, $\epsilon_2 = 0$)**	**Rotation ($\epsilon_1 = 0$, $\epsilon_2 = 0$)**
Josephson Junction ($\mathcal{M}_1$)	$\dot{\phi}_i = y_i$ $\dot{y}_i = I - \alpha\, y_i - \sin\phi_i +$ $\epsilon_1 \sum_j A_{ij}(\phi_j - \phi_i) + \epsilon_2 \sum_j A_{ij}(y_j - y_i)$	$I > 1, \alpha > 0$		No	Yes
VCON ($\mathcal{M}_2$)	$\dot{\phi}_i = y_i$ $\dot{y}_i = I - \beta y_i(y_i^2 - \alpha) - \sin\phi_i +$ $\epsilon_1 \sum_j A_{\iota j}(\phi_j - \phi_\iota) + \epsilon_2 \sum_j A_{\iota j}(y_j - y_\iota)$	$I = 0.5$, $\beta = 0.5$	$\alpha > 0.84$	No	Yes
			$\alpha < 0.84$	Yes	No
			$\alpha \approx 0.84$ (Bistable)	Yes	Yes

FIG. 1. Globally coupled networks under phase and phase velocity interactions. $\mathcal{M}_1$: A classical Josephson junction model. $\mathcal{M}_2$: VCON model. $\mathcal{M}_1$ reveals the rotation for the choice of I and α ($I = 1.5$). In $\mathcal{M}_2$, the parameter α determines the transition of the attractor from libration to rotation for a range of β and I values. ϵ_1 and ϵ_2 represent diffusive phase coupling and diffusive phase velocity coupling, respectively. A_{ij} denotes the adjacency matrix of the networks; in our present case, all nodes are all-to-all coupled, i.e., $A_{ij} = 1$ if $i \neq j$. ϕ_i and y_i are the phase and phase velocity variables in both models.

libration [1,2,14,21], to confirm the generality of our results. Our result suggests that if the uncoupled system is in librational (rotational) motion, the phase coupling should be negative (positive). The contrasting effect emerges if the oscillators are connected by phase velocity variables. This particular effect is not system specific but rather related to the coupling framework of the autonomous second-order phase models that exhibit libration or rotation depending on the system parameters.

Network models. We consider globally coupled networks of two model systems with distributed parameters and explore the effect for two different coupling configurations (phase and phase velocity), separately. The model systems, namely the Josephson junction ($\mathcal{M}_1$) and voltage-controlled oscillations in neurons ($\mathcal{M}_2$), are used to form the networks. The networks using $\mathcal{M}_1$ and $\mathcal{M}_2$ models are described in Fig. 1. A single Josephson junction ($\mathcal{M}_1$) usually shows rotation on a cylindrical surface alike an inverted pendulum for a broad range of parameters [32], but on occasion, especially in the coupled state [5], may show libration as a simple pendulum with a to-and-fro small oscillation. In libration, the trajectory never encircles the cylindrical surface although it lives on the surface. The network with VCON node dynamics ($\mathcal{M}_2$) has an almost similar mathematical description, but with an additional cubic nonlinearity controlled by β, and α is the coefficient of a linear function. This model is related to the neuronal membrane dynamics [33,34], however, we are not interested here in its neural properties. A variation of a system parameter (α) can easily transform the system from libration to rotation as given in Fig. 1. This helps us explore the contrarian role of phase and phase velocity coupling on synchrony with changes in specific dynamics. Here, the phase velocity $\dot{\theta}$ represents the membrane potential of neurons. For a suitable choice of parameters, the system shows rich complex behavior—the existence of a saddle point, an unstable spiral, a stable limit cycle (libration, restricted to one sheet of a cylinder), and a stable running periodic solution (rotational motion)—thus revealing subthreshold and superthreshold neuronal oscillations.

We consider globally coupled networks of the two models, separately, with a distribution of α and an appropriate choice of other fixed parameters of both systems. First, we define an order parameter r (where $re^{i\Theta} = \frac{1}{N}\sum_{j=1}^{N} e^{i\phi_j}$) as a function of phase coupling ($\epsilon_1 \neq 0$, $\epsilon_2 = 0$) as well as phase velocity coupling ($\epsilon_1 = 0$, $\epsilon_2 \neq 0$) and numerically calculate it to explore the synchronization processes. Positive phase coupling ($\epsilon_2 = 0$) is a necessity for the second-order transition to phase coherence as shown in Fig. 2(a) for both the network models (yellow and blue lines) as usual. An opposite scenario appears in Fig. 2(b) when only the phase velocity coupling ($\epsilon_1 = 0$) is considered. Note that, for the calculation of r, the parameters of both the isolated models are chosen such that the dynamics are in rotation.

Next, we search for the stability conditions for complete synchrony and explore the contrarian roles of phase and phase velocity coupling in identical networks. A semianalytical approach [19] is adopted for deriving the stability conditions of complete synchrony for both the model networks, thereby demarcating the synchronized and desynchronized regions in the coupling parameter plane. For the $\mathcal{M}_1$ system, the globally coupled network with diffusive phase and phase velocity coupling is described for an arbitrary kth node,

$$\ddot{\phi}_k + \alpha\dot{\phi}_k + \sin\phi_k = I + \frac{\epsilon_1}{N}\sum_{j=1}^{N}(\phi_j - \phi_k) + \frac{\epsilon_2}{N}\sum_{j=1}^{N}(\dot{\phi}_j - \dot{\phi}_k). \quad (1)$$

The time evolution of phase ϕ and $\ddot{\phi}$ variables is controlled [7] by the damping parameter α and a constant bias I. We remind here that this network model represents the dynamics of the superconducting Josephson arrays where the phase ϕ_k is connected with the supercurrent and the phase velocity $\dot{\phi}_k = y_k$ appears as the voltage across the kth junction ($\mathcal{M}_1$), and it is proportional to the frequency of oscillation [3]. For $I > 1$, the isolated system is in rotation on the $\dot{\phi} - \phi$ cylindrical surface. In a completely synchronized state of the array, all of the junctions oscillate in unison when the synchronization manifold is defined by $\phi_k = \phi_0$. In the synchronous state, the N-dimensional system is reduced to

$$\ddot{\phi}_0 + \alpha\dot{\phi}_0 + \sin\phi_0 = I. \quad (2)$$

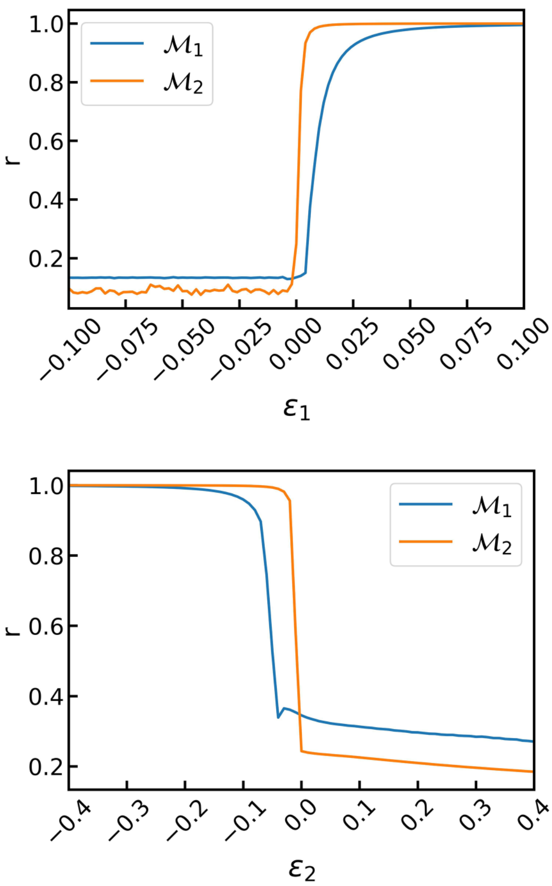

FIG. 2. Emergent synchrony in globally coupled networks. Order parameter r against (a) phase coupling $\epsilon_1 \neq 0$ ($\epsilon_2 = 0$) and (b) phase velocity coupling $\epsilon_2 \neq 0$ ($\epsilon_1 = 0$). A Cauchy or Lorentz distribution of α is considered around $\alpha = 1.5$, and $I = 1.5$ for the system $\mathcal{M}_1$. On the other hand, a similar Cauchy or Lorentz distribution of α is considered around $\alpha = 0.95$ for the second system $\mathcal{M}_2$; other parameters are $I = 0.5$ and $\beta = 0.5$. Positive coupling is required for phase coherence. An opposite scenario appears in (b) where phase velocity coupling ($\epsilon_1 = 0$, $\epsilon_2 \neq 0$) is introduced, and phase coherence emerges for a negative ϵ_2. Note that, for calculating the order parameter r, the parameters of both the isolated models are chosen such that the dynamics is rotational. Network size: $N = 100$ nodes.

To derive the stability of complete synchrony, we apply a small perturbation, $\phi_k = \phi_0 + \eta_k$, and linearize around the synchronized state ϕ_0,

$$\ddot{\eta}_k + \alpha\dot{\eta}_k + \cos\phi_0\eta_k = \frac{\epsilon_1}{N}\sum_{j=1}^{N}(\eta_j - \eta_k) + \frac{\epsilon_2}{N}\sum_{j=1}^{N}(\dot{\eta}_j - \dot{\eta}_k) \tag{3}$$

$$\Rightarrow \ddot{\eta}_k + (\alpha + \epsilon_2)\dot{\eta}_k + (\cos\phi_0 + \epsilon_1)\eta_k = \frac{\epsilon_1}{N}\sum_{j=1}^{N}\eta_j + \frac{\epsilon_2}{N}\sum_{j=1}^{N}\dot{\eta}_j. \tag{4}$$

There is permutation symmetry in the system. Any permutation $\eta_j \leftrightarrow \eta_k$ leaves this equation unchanged. Considering the transformation with mean coordinate $v = \frac{1}{N}\sum_{j=1}^{N}\eta_k$ and $(N-1)$ relative coordinates $\zeta_k = \eta_k - \eta_{k+1}$, we can write Eq. (4),

$$\ddot{\zeta}_k + (\alpha + \epsilon_2)\dot{\zeta}_k + (\cos\phi_0 + \epsilon_1)\zeta_k = 0. \tag{5}$$

We simulate Eqs. (2) and (5) simultaneously and derive where the relative errors ζ_k decay to zero in ϵ_1-ϵ_2 space that demarcates the region of stable synchrony.

A similar semianalytical approach is adopted for a globally coupled network with the node dynamics of $\mathcal{M}_2$. The transformed equation of the relative errors appears,

$$\ddot{\zeta}_k + \left(3\beta\dot{\phi}_0^2 - \alpha\beta + \epsilon_2\right)\dot{\zeta}_k + (\cos\phi_0 + \epsilon_1)\zeta_k = 0. \tag{6}$$

We simulate Eq. (6) together with the coherent solution,

$$\ddot{\phi}_0 + \beta\dot{\phi}_0\left(\dot{\phi}_0^2 - \alpha\right) + \sin\phi_0 = I. \tag{7}$$

(See Supplemental Material [35] for a detailed analysis.)

The regions of synchrony (yellow color) and desynchrony (orange color) are illustrated in the ϵ_1-ϵ_2 coupling parameter plane in Fig. 3 for the two networks. A stable synchronization line (dashed line) is drawn as obtained using the semianalytical approach for both models that marks the separating line between the synchronous and asynchronous regions. For the network with the $\mathcal{M}_1$ model, the regular graph ($N = 100$) emerges into complete synchrony (yellow region) for $\epsilon_2 < 0$ when the transition occurs at a critical value along the vertical line ($\epsilon_1 = 0$) as shown in Fig. 3(a). The network is desynchronized (orange region) for $\epsilon_2 > 0$ ($\epsilon_1 = 0$). The corresponding trajectories of all the units (color circles) are shown on a y-ϕ cylindrical plane immediately below each phase diagram of the ϵ_1-ϵ_2 plane. In the desynchronized state, the dynamical units are in rotation on the cylindrical surface. They are distributed in phase space during desynchrony, but converge to one cluster (red circle), rotating once again on the cylindrical surface when synchronized. Of course, there exists a broad region of synchrony (yellow) for $\epsilon_1 \neq 0$ and $\epsilon_2 \neq 0$ when both the phase velocity and phase coupling are active, however, it is not the main focus of our work. For a regular graph with dynamical units using the model $\mathcal{M}_2$, a similar synchronization scenario is seen in Fig. 3(b), when the individual units are also in rotation for $\alpha > 0.84$ ($\beta = 0.5$ and $I = 0.5$). Synchrony emerges at a critical negative value of phase velocity coupling ($\epsilon_1 = 0$). The corresponding trajectories once again confirm the scenarios on the cylindrical surface either as distributed (asynchronous) or convergent (synchronous) in rotation. Figure 3(c) shows the opposite picture of collective dynamics, when the model $\mathcal{M}_2$ in isolation is in libration for $\alpha < 0.84$. A broad parameter space in the ϵ_1-ϵ_2 plane exists where we find complete synchrony (yellow) delineated from the desynchronized region (orange) by the semianalytical stability line (dashed line). Positive phase velocity coupling ($\epsilon_1 = 0$) is a necessity for synchrony, otherwise, negative phase coupling ($\epsilon_2 = 0$) is necessary to achieve synchrony. The trajectories are plotted below for both the synchronous and asynchronous states in a cylindrical plane. The trajectories make a small cycle, but never rotate around the cylindrical surface that indicates their libration. The whole scenario is further clarified in a phase diagram in Fig. 4 that shows regions of rotation and libration in the dynamics of the $\mathcal{M}_2$ and the corresponding collective dynamics. There exists a region of synchrony (yellow) of the network under phase velocity coupling $\epsilon_2 < 0$

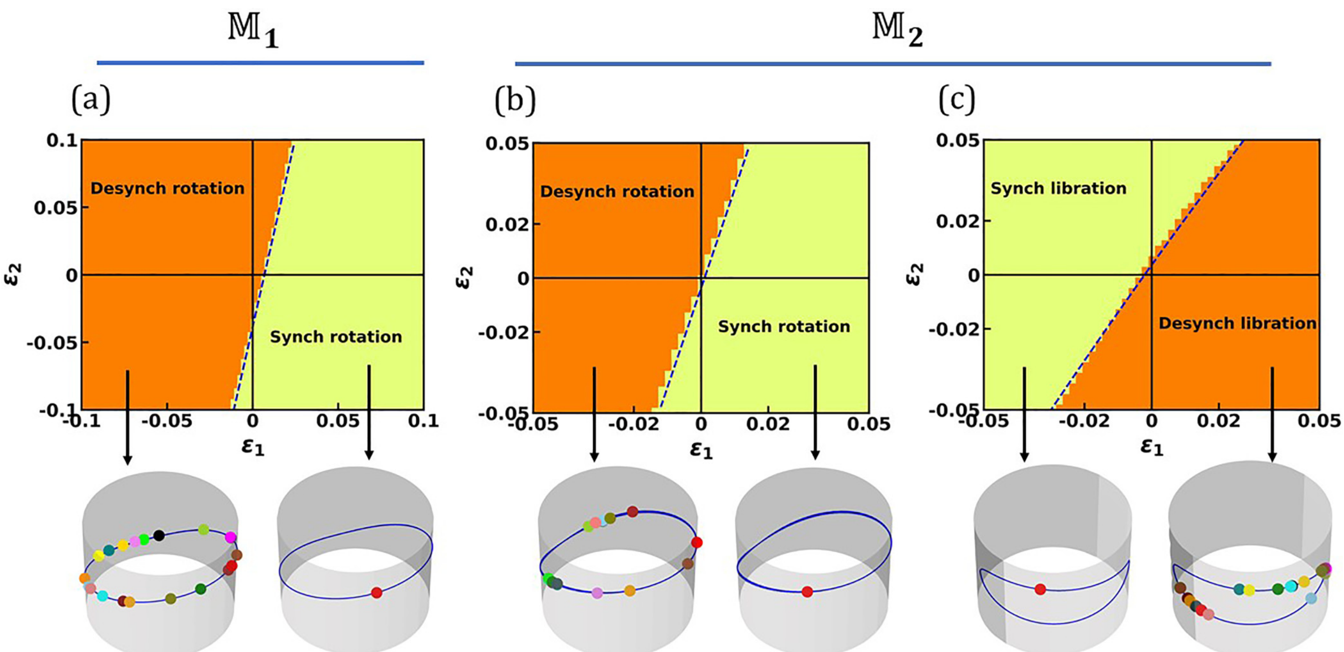

FIG. 3. Phase diagram in an ϵ_1-ϵ_2 plane. The synchronization region is shown in yellow color and desynchronization in orange. The dashed line represents the semianalytical line for stable synchronization. This line separates the synchronization phase space from the desynchronization phase space. (a) Model $\mathcal{M}_1$: For $\epsilon_1 = 0$ (vertical black line), the regular graph emerges into complete synchronization for $\epsilon_2 < 0$. An exactly opposite scenario occurs, when $\epsilon_2 = 0$ (horizontal black line). (b) Model $\mathcal{M}_2$: It shows a scenario similar to (a), when the individual units are in rotation ($I = 0.5$, $\alpha > 0.84$, $\beta = 0.5$). (c) Model $\mathcal{M}_2$: The scenario is reversed when the individual units are in libration ($I = 0.5$, $\alpha < 0.84$, $\beta = 0.5$). The corresponding trajectories of all the emergent states are illustrated in cylindrical phase space immediately below each phase diagram and for synchronization (all oscillators in color circles converge into one, in rotation or libration) and desynchronization (all oscillators in color circles are distributed along the trajectories, in rotation or libration) regimes. Number of globally coupled oscillators: $N = 100$.

($\epsilon_1 = 0$) when the system is in rotation ($\alpha > 0.84$). The network needs positive phase velocity coupling $\epsilon_2 > 0$ for synchrony (yellow region) when the individual units are in libration for $\alpha < 0.84$. A bistable region (blue color) exists where synchronous and asynchronous regimes coexist and appear as depending on the initial conditions.

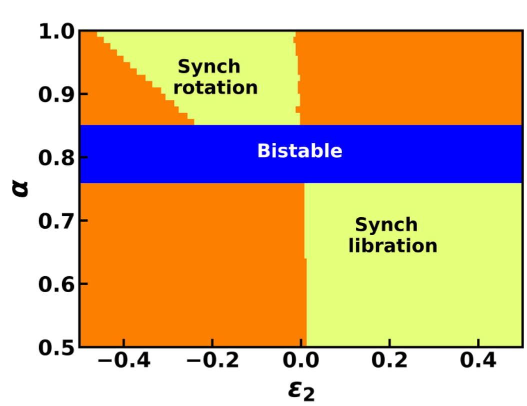

FIG. 4. Phase diagram in an α-ϵ_2 plane. Emergent dynamics in a globally coupled network of the $\mathcal{M}_2$ model system. Synchronous (yellow) and desynchronous (orange) regimes are demarcated. The isolated nodes are in rotation ($\alpha > 0.84$). The system is purely in libration ($\alpha < 0.8$). A bistable region (blue color) of the system dynamics exists where no such synchrony is possible, where synchrony and asynchrony coexist.

Mechanism. The results raise a pertinent question: Why is negative phase velocity (or positive phase) coupling essential for the synchronization of connected second-order phase oscillators that resemble pendula dynamics with rotational motion? From a mathematical standpoint, our semianalytical approach provides a solution [see Eqs. (6) and (7) for the VCON model]. To delve deeper, we analyze Eq. (6) as a damped simple harmonic oscillator, by assuming that the coefficient of the damping term is constant, i.e., $(3\beta\dot{\phi}_0^2 - \alpha\beta + \epsilon_2)$ is not a function of t. Thus, $\dot{\phi}_0^2$ which is coming from the time-dependent solution of Eq. (7) should be considered as time independent. With this approximation, we take the average of $\dot{\phi}_0^2$ in time. On the other hand, we also treat the frequency term $(\cos\phi_0 + \epsilon_1)$ as constant by substituting $\cos\phi_0$ with its average value. Note that changing the parameter α_0 will change the solution of the uncoupled VCON model [Eq. (7)], leading to rotational motion from the librational dynamics. Therefore, the strength of the damping and frequency terms will also change. Accumulating all the information, we show that $\epsilon_{1c} = \frac{1}{4}[3\beta(\dot{\phi}_0)^2_{\text{avg}} - \alpha\beta]^2 - (\cos\phi_0)_{\text{avg}}$, and $\epsilon_{2c} = 2\sqrt{(\cos\phi_0)_{\text{avg}}} + \alpha\beta - 3\beta(\dot{\phi}_0)^2_{\text{avg}}$. Clearly, if $(\dot{\phi}_0)^2_{\text{avg}}$ is too high (that is the case for rotation), the phase velocity coupling ϵ_{2c} will be negative. The contrasting effect occurs for the phase coupling ϵ_{1c}. For more details, please see the Supplemental Material [35]. A similar argument also explains the collective dynamics for the Josephson junction arrays in rotation. We acknowledge that the analysis is carried out with some approximations (damping coefficient and frequency are assumed constants) and thereby try to develop an understanding of why the counterintuitive phenomenon happens, although the exact mechanism is still elusive.

Conclusion. An ensemble of phase oscillators transits from a disordered state to an ordered phase coherent state for positive coupling that has been necessarily defined by pure phase coupling. Positive coupling attracts the phase oscillators to converge into one cluster. A network of chaotic oscillators (identical or distributed parameters) also follows a similar trend of transition for positive coupling via the state variables. Both the phase and amplitude are imbibed in the state variables and in the definition of the coupling function. As usual, positive phase coupling or the coupling via the state variables (amplitude and phase coupling in combination) thus attracts different trajectories of the dynamical nodes to converge into a coherent state. This conventional concept of the attractive nature of positive coupling using simply phase variables or the state variables of limit cycle systems is reversed for pure phase velocity coupling, when the phase velocity variable happens to appear separately from the phase variable in dynamical systems. The oscillators can synchronize only for negative phase velocity coupling. We have extended here our previous results [16,20] on a network of Josephson junctions that represents a second-order phase dynamics and shows rotational dynamics for a broad range of parameters. We confirm this scenario using another VCON model to form a regular graph and explore the transition to synchrony for identical and nonidentical cases. This VCON model shows both rotation and libration for a change of parameters. Thereby, we come to a conclusion that synchronization emerges in an ensemble of second-order phase oscillators in rotation for negative phase velocity coupling. Positive phase velocity (or negative phase) coupling plays an attractive role for the oscillators in libration to emerge into a coherent state. Recently, the role of contrarians has been explored in the synchrony of phase oscillators under higher-order interactions [36] and chaotic oscillators under cross-repulsive coupling [37–40], however, none of them focused specifically on phase velocity coupling. We delineate here the contrarian roles of phase velocity and phase coupling on synchrony in oscillators where the phase and phase velocity appear as separate variables. For physical devices such as the Josephson junction, phase velocity coupling appears as voltage across the junction and it has an important role in the collective dynamics of the arrays of junctions for practical purposes.

All data are available for free on request from the authors.

Acknowledgment. C.H. is supported by a DST-INSPIRE-Faculty grant (Grant No. IFA17-PH193).

[1] Y. Braiman, J. F. Lindner, and W. L. Ditto, Taming spatiotemporal chaos with disorder, Nature (London) **378**, 465 (1995).

[2] A. Gavrielides, T. Kottos, V. Kovanis, and G. P. Tsironis, Spatiotemporal organization of coupled nonlinear pendula through impurities, Phys. Rev. E **58**, 5529 (1998).

[3] B. Josephson, Possible new effects in superconductive tunnelling, Phys. Lett. **1**, 251 (1962).

[4] W. C. Stewart, Current-voltage characteristics of Josephson junctions, Appl. Phys. Lett. **12**, 277 (1968).

[5] A. Ray, A. Mishra, D. Ghosh, T. Kapitaniak, S. K. Dana, and C. Hens, Extreme events in a network of heterogeneous Josephson junctions, Phys. Rev. E **101**, 032209 (2020).

[6] D. E. McCumber, Effect of ac impedance on dc voltage-current characteristics of superconductor weak-link junctions, J. Appl. Phys. **39**, 3113 (1968).

[7] M. Levi, F. C. Hoppensteadt, and W. L. Miranker, Dynamics of the Josephson junction, Quart. Appl. Math. **36**, 167 (1978).

[8] S. K. Dana, D. C. Sengupta, and K. D. Edoh, Chaotic dynamics in Josephson junction, IEEE Trans. Circuits Syst. I **48**, 990 (2001).

[9] S. K. Dana, D. C. Sengupta, and C.-K. Hu, Spiking and bursting in Josephson junction, IEEE Trans. Circuits Syst. II **53**, 1031 (2006).

[10] A. Mishra, S. Ghosh, S. K. Dana, T. Kapitaniak, and C. Hens, Neuron-like spiking and bursting in Josephson junctions: A review, Chaos **31**, 052101 (2021).

[11] P. Jaros, S. Ghosh, D. Dudkowski, S. K. Dana, and T. Kapitaniak, Higher-order interactions in Kuramoto oscillators with inertia, Phys. Rev. E **108**, 024215 (2023).

[12] D. Chalkiadakis and J. Hizanidis, Dynamical properties of neuromorphic Josephson junctions, Phys. Rev. E **106**, 044206 (2022).

[13] J. Rubinstein, Sine-Gordon equation, J. Math. Phys. **11**, 258 (1970).

[14] S. F. Brandt, B. K. Dellen, and R. Wessel, Synchronization from disordered driving forces in arrays of coupled oscillators, Phys. Rev. Lett. **96**, 034104 (2006).

[15] C. Yao, M. Zhan, J. Shuai, J. Ma, and J. Kurths, Insensitivity of synchronization to network structure in chaotic pendulum systems with time-delay coupling, Chaos **27**, 126702 (2017).

[16] S. Saha and S. K. Dana, Smallest chimeras under repulsive interactions, Front. Netw. Physiol. **1**, 778597 (2021).

[17] K. Wiesenfeld and P. Hadley, Attractor crowding in oscillator arrays, Phys. Rev. Lett. **62**, 1335 (1989).

[18] S. H. Strogatz and R. E. Mirollo, Splay states in globally coupled Josephson arrays: Analytical prediction of Floquet multipliers, Phys. Rev. E **47**, 220 (1993).

[19] P. Hadley, M. R. Beasley, and K. Wiesenfeld, Phase locking of Josephson-junction series arrays, Phys. Rev. B **38**, 8712 (1988).

[20] A. Mishra, S. Saha, and S. K. Dana, Chimeras in globally coupled oscillators: A review, Chaos **33**, 092101 (2023).

[21] A. Ray, T. Bröhl, A. Mishra, S. Ghosh, D. Ghosh, T. Kapitaniak, S. K. Dana, and C. Hens, Extreme events in a complex network: Interplay between degree distribution and repulsive interaction, Chaos **32**, 121103 (2022).

[22] Y. Kuramoto, in *International Symposium on Mathematical Problems in Theoretical Physics*, edited by H. Araki, Lecture Notes in Physics Vol. 39 (Springer, Berlin, 1975), p. 420.

[23] L. M. Pecora and T. L. Carroll, Synchronization in chaotic systems, Phys. Rev. Lett. **64**, 821 (1990).

[24] L. M. Pecora and T. L. Carroll, Master stability functions for synchronized coupled systems, Phys. Rev. Lett. **80**, 2109 (1998).

[25] M. G. Rosenblum, A. S. Pikovsky, and J. Kurths, Phase synchronization of chaotic oscillators, Phys. Rev. Lett. **76**, 1804 (1996).

[26] L. M. Pecora, T. L. Carroll, G. A. Johnson, D. J. Mar, and J. F. Heagy, Fundamentals of synchronization in chaotic systems, concepts, and applications, Chaos **7**, 520 (1997).

[27] S. Boccaletti, J. Kurths, G. Osipov, D. L. Valladares, and C. S. Zhou, The synchronization of chaotic systems, Phys. Rep. **366**, 1 (2002).

[28] A. Pikovsky, M. Rosenblum, and J. Kurths, *Synchronization: A Universal Concept in Nonlinear Science* (Cambridge University Press, Cambridge, UK, 2002).

[29] H. Hong and S. H. Strogatz, Kuramoto model of coupled oscillators with positive and negative coupling parameters: An example of conformist and contrarian oscillators, Phys. Rev. Lett. **106**, 054102 (2011).

[30] Y. Kuramoto, *Chemical Oscillations, Waves, and Turbulence* (Springer-Verlag, Berlin, 1984).

[31] M. Rosenblum and J. Kurths, *Synchronization: A Universal Concept in Nonlinear Science* (Cambridge University Press, Cambridge, UK, 2003).

[32] A. Mishra, S. Saha, C. Hens, P. K. Roy, M. Bose, P. Louodop, H. A. Cerdeira, and S. K. Dana, Coherent libration to coherent rotational dynamics via chimeralike states and clustering in a Josephson junction array, Phys. Rev. E **95**, 010201(R) (2017).

[33] F. Hoppensteadt, Voltage-controlled oscillations in neurons, Scholarpedia **1**, 1599 (2006).

[34] F. Hoppensteadt, Biologically inspired circuits: Coalition formation in aggregates, Int. J. Bifurcation Chaos **16**, 3349 (2006).

[35] See Supplemental Material at http://link.aps.org/supplemental/10.1103/PhysRevE.108.L042201 for a detail description of the network of VCON model and the Josephson junctions, and the stability conditions of synchronization for both the models, which includes Refs. [41,42].

[36] K. Kovalenko, X. Dai, K. Alfaro-Bittner, A. M. Raigorodskii, M. Perc, and S. Boccaletti, Contrarians synchronize beyond the limit of pairwise interactions, Phys. Rev. Lett. **127**, 258301 (2021).

[37] S. Mirzaei, Md. Sayeed Anwar, F. Parastesh, S. Jafari, and D. Ghosh, Synchronization in repulsively coupled oscillators, Phys. Rev. E **107**, 014201 (2023).

[38] S. Saha, A. Mishra, E. Padmanaban, S. K. Bhowmick, P. K. Roy, B. Dam, and S. K. Dana, Coupling conditions for globally stable and robust synchrony of chaotic systems, Phys. Rev. E **95**, 062204 (2017).

[39] S. Saha, Resilience in multiplex networks by addition of cross-repulsive links, IEEE Trans. Netw. Sci. Eng. **9**, 1594 (2022).

[40] S. Saha, A. Mishra, P. K. Roy, and S. K. Dana, Cross-coupling plays constructive role on global stability of synchrony in neuronal networks, Opera Med. Physiol. **3**, 93 (2017).

[41] S. I. Hayek, Mechanical vibration and damping, in *Digital Encyclopedia of Applied Physics* (Wiley-VCH, Weinheim, 2003).

[42] E. Kreyszig, *Advanced Engineering Mathematics* (Wiley, New York, 1983).